Interconnectedness and Banking Performance: Insights from the Interbank Lending Market in Chile *

Luis Chanci Subal C. Kumbhakar Paulo Bobadilla

(This version: December 2025. Comments are welcome.)

Abstract

Financial networks are typically studied for their role in propagating shocks, yet much less is known about how these linkages shape banks' routine operational performance. This paper examines whether interconnectedness in the interbank lending market affects cost efficiency. Using confidential administrative data from the Chilean banking sector (2008–2020), we map the "physical" network of bilateral exposures and estimate a network-augmented stochastic cost frontier through a two-step GMM framework adapted to the multi-output structure of banking. We find that interconnectedness is a statistically significant determinant of performance. Specifically, we estimate a negative network dependence parameter, suggesting that stronger network ties are associated with higher cost efficiency in the Chilean market. Decomposing total inefficiency, we find that network effects account for a median reduction of approximately 35 percentage points in cost inefficiency relative to the idiosyncratic component. These results provide novel empirical evidence that interbank networks influence not only the propagation of financial shocks but also the underlying operational performance of banks. The findings highlight the importance of monitoring the structure of financial networks as a key element of both stability analysis and performance evaluation.

JEL codes: G21, D24, C23, L14, G01.

Keywords: Banking Interconnections, Interbank Market, Cost Efficiency, Peer Effects, Chile.

*Notes: (1) The regulatory authority of Chile, *Comisión para el Mercado Financiero* (CMF), kindly provided data through the Call for Research Projects 2024. The views, findings, and conclusions expressed herein are solely those of the authors and do not necessarily represent those of the CMF. All errors and omissions are the responsibility of the authors. (2) This research has benefited greatly from the valuable feedback of Sofía Bauducco and participants at the CMF Annual Meeting and the Encuentro de la Sociedad de Economía Chilena (SECHI). Luis Chanci gratefully acknowledges financial support from the Agencia Nacional de Investigación y Desarrollo (ANID) through the Fondecyt Iniciación en Investigación project No. 11250893. (3) Contact information. Luis: Universidad Santo Tomás, Chile, *luischanci@santotomas.cl*; Subal: Binghamton University, USA, *kkar@binghamton.edu*; Paulo: CMF, Chile, *pbobadilla@cmfchile.cl*.

1 Introduction

Financial system outcomes emerge primarily from interaction patterns rather than isolated institutional behavior. In banking, the configuration of interbank linkages shapes how information, liquidity, and shocks propagate, with implications extending far beyond systemic fragility to potentially shape routine operational performance. However, while existing research and policy debates prioritize stability and risk contagion, considerably less attention has been devoted to how interconnectedness influences banks' performance and productivity during periods of relative calm. This paper examines whether the structure of interbank lending relationships affects cost performance. Specifically, we ask: does interconnectedness, defined by interbank lending network structures, systematically influence operational cost efficiency?

Network ties may act as conduits for strategic interaction and information flow. First, imitation and herding mechanisms may enable banks to economize on information acquisition costs. Second, direct connections can facilitate social learning, allowing banks to benchmark their efficiency against the operational successes or failures of their counterparties. Finally, the broader network topology may influence market power and the diffusion speed of best practices. Through these potential channels, interconnectedness not only propagates risk but may also shape the cost structure of the banking sector.

Despite plausible theoretical foundations, empirical evidence linking interbank relationships to broader banking performance remains limited. This gap stems from both data and methodological challenges. Granular data that traces specific bilateral linkages, crucial for mapping the transmission of shocks to individual balance sheets, is typically confidential and difficult to access. Consequently, prior research has often relied on aggregation, simulations, or imperfect proxies like geographical distance, which often obscure the true topology of financial interdependence. Furthermore, identifying causal effects on efficiency within complex endogenous networks poses econometric challenges that standard models often fail to mitigate.

To overcome these empirical challenges, we leverage a unique administrative dataset from the Chilean banking sector alongside advanced efficiency modeling techniques. The data, obtained directly from the financial market regulator[1], include detailed transaction records from the interbank lending market (Form C-18) linked with monthly balance sheets and other bank-level controls for nearly all institutions operating in the country between 2008 and 2020. This rich panel, based on observed lending relationships rather than correlation-based proxies, enables us to construct network adjacency matrices that accurately capture the intensity and relevance of interbank connections.

Methodologically, we employ a two-step Generalized Method of Moments (GMM) estimation approach, building on recent advances in stochastic frontier (SF) analysis with spatial dependencies (e.g., Hou et al., 2023; Chanci et al., 2024). We specify the SF model as a stochastic cost frontier, consistent with the assumption of cost-minimizing behavior in banking institutions. Unlike standard spatial approaches that proxy connectivity using geographic distance, our analysis incorporates weighting matrices derived from interbank lending data to measure financial interdependence directly. This strategy allows us to estimate bank-level cost efficiency using a flexible translog specification that explicitly accounts for interbank network structures while controlling for unobserved heterogeneity.

[1] The *Comisión para el Mercado Financiero* (CMF).

Our empirical analysis centers on the network dependence parameter (ρ), which quantifies the equilibrium relationship between a bank's operational efficiency and that of its counterparties. We interpret this parameter through the lens of the social interaction literature, specifically targeting the endogenous peer effect described by Manski (1993). Identifying such effects is inherently difficult due to the "reflection problem," where observed correlations in outcomes may stem from similarities in characteristics (contextual effects) or exposure to common shocks (correlated effects) rather than direct influence. Our two-step estimation strategy is designed to mitigate these confounding factors. First, the stochastic cost frontier conditions on a comprehensive set of bank-specific cost drivers, including output mix, input prices, and risk capital, alongside time-fixed effects. This step effectively purges the inefficiency term of observable contextual variation and aggregate common shocks before network dependence is estimated. Second, the GMM estimator leverages the distinct, non-universal topology of the interbank network to identify ρ from the moment conditions of the variance-covariance structure. Consequently, while we interpret the results with caution given the lack of exogenous variation from a natural experiment, this framework isolates a robust measure of endogenous network dependence that is distinct from simple sorting or environmental correlations.

The results indicate that the Chilean banking system operates with relatively high levels of cost efficiency, and that these outcomes are systematically influenced by interbank linkages. The estimated network dependence parameter ($\hat{\rho} \approx -0.5$) is negative, suggesting that ties in the interbank lending network correspond, on average, to lower inefficiency (i.e., higher cost efficiency). To assess the economic magnitude of this relationship, we decompose total inefficiency into its idiosyncratic and network-related components. We find that the network component reduces inefficiency by approximately 35 percentage points for the median bank, relative to its idiosyncratic component. These findings align with mechanisms such as benchmarking or information diffusion within the network. Overall, the evidence highlights that understanding and monitoring interbank network dynamics is relevant not only for assessing systemic fragility but also for evaluating the operational performance that supports broader economic functioning.

The contributions of this research are threefold. First, it provides direct empirical evidence linking actual interbank networks to operational performance, bridging the gap between the banking literature and the limited empirical evidence on peer effects within financial institutions. In doing so, the analysis moves beyond the traditional focus on systemic risk and contagion to examine how network structures relate to banks' cost efficiency during normal times. Second, methodologically, we extend the network-augmented stochastic frontier framework to a *cost minimization* setting. While recent advances in this literature have focused on production functions (e.g., Hou et al., 2023), our cost-based specification is better suited to the multi-output nature of banking and to an industry where costs, rather than output quantities, constitute the primary optimization margin. In doing so, we extend the application of network SF models to a context that more accurately reflects the technological and operational realities of financial institutions. Third, we exploit a unique regulatory dataset containing complete bilateral exposures across the Chilean interbank market. This enables us to map the actual network of lending relationships, distinguishing our approach from empirical works that rely on proxies such as geographic distance or correlational measures based on forecast error variance decompositions from Vector Autoregressive (VAR) models. This level of granularity overcomes common data limitations in the banking network literature and provides a more

accurate foundation for identifying how interbank structures relate not only to systemic risk but also to fundamental aspects of operational efficiency.

The remainder of this section reviews the related literature. The rest of the paper is organized as follows: Section 2 presents our proposed econometric framework, detailing the shift from the standard production frontier model with geographical interdependence to a cost minimization specification that accounts for network structures. Section 3 describes the unique administrative dataset and the construction of the variables, paying particular attention to the formulation of the adjacency matrix. Section 4 reports the empirical findings, including the parameter estimates and a decomposition analysis that isolates the network contribution to efficiency. Section 5 discusses the broader implications of these results and concludes.

Related literature Our paper relates to and contributes to several distinct strands of literature. First, we contribute to the extensive body of work examining financial interconnectedness. Foundational theoretical contributions, such as Allen and Gale (2000) and Freixas et al. (2000), established that while interbank linkages provide essential insurance against idiosyncratic liquidity shocks, they simultaneously create channels for contagion that can destabilize the system. This literature, heavily influenced by the 2007–2009 global financial crisis, has largely focused on the structural fragility of networks and their role in propagating systemic risk (Jackson and Pernoud, 2021; Glasserman and Young, 2016). A central theme in this strand of research is the inherent trade-off between risk-sharing and contagion, often described as the "robust-yet-fragile" property of financial networks. For instance, Acemoglu et al. (2015) and Elliott et al. (2014) formally show that while denser connectivity facilitates diversification and absorption of small shocks, it also serves as a mechanism for cascading failures when shocks exceed a certain magnitude. Similarly, **?** highlight how greater connectivity can increase the probability of systemic collapse during stress events. While we build on the premise that network structure fundamentally alters bank outcomes, our study diverges from this stability-centric focus. Instead of examining how networks amplify extreme tail events (crises), we empirically explore how these structures influence a critical but less-studied economic outcome: banking operational performance and cost efficiency during periods of relative stability.

Second, our work contributes to the literature on peer effects and social learning in finance. Drawing on the identification framework of Manski (1993), this strand of research posits that economic agents, including banks, imitate peers to economize on information acquisition costs or to leverage perceived superior expertise. The theoretical foundations of such behavior are well-established: Scharfstein and Stein (1990) and Bikhchandani et al. (1998) describe how reputational concerns and informational cascades can lead rational agents to ignore private signals in favor of the aggregate consensus (see also Banerjee, 1992). Empirically, evidence of such dynamics in the banking sector is growing but limited. Notable exceptions include **?**, who identifies spillover effects in foreclosure decisions using quasi-random variation in bankruptcy courts, and Margaretic et al. (2021), who document peer effects in the Chilean interbank market, showing that banks mimic their peers' decisions to cut credit lines to stressed institutions.

We extend this literature by shifting the focus from behavioral contagion to operational performance. While studies like Margaretic et al. (2021) primarily analyze how peer interactions drive lending decisions

or risk avoidance, our research examines how these interconnections shape a fundamental economic outcome: cost efficiency. We depart from standard approaches by integrating interconnectedness directly into a stochastic frontier econometric model. This allows us to move beyond detecting the presence of herding to quantifying the economic magnitude of network spillovers on banking productivity.

Third, our research contributes to the literature linking network structures to banking performance (e.g., Silva et al., 2018, 2016; Elliott et al., 2014). This literature suggests several channels through which interconnectedness can enhance operational efficiency, including improved liquidity management, specialization, and the accelerated diffusion of information or technology. However, empirical evidence quantifying these effects remains limited. A notable exception is Silva et al. (2016), who examine the Brazilian interbank market to understand how network topology, specifically core-periphery structures, affects bank performance. Their approach is two-step: they first estimate efficiency scores using stochastic frontier analysis and subsequently regress these scores on network metrics. They find that a bank's position in the core is positively associated with cost efficiency but negatively associated with risk-taking efficiency. Our study fundamentally departs from this approach by moving beyond topological statistics. Rather than using aggregated measures (such as centrality) as explanatory variables for pre-estimated efficiency, we incorporate network dependencies directly into the error structure of the stochastic cost frontier via the full adjacency matrix. This allows us to model a direct transmission mechanism: how a bank's operational inefficiency is contemporaneously influenced by the inefficiency of its actual counterparties. By treating the network as a channel for endogenous spillovers rather than just a set of structural characteristics, we offer a more granular and structurally grounded assessment of how interbank relationships shape performance.

Fourth, we contribute to the debate on network measurement by distinguishing between 'physical' and 'statistical' interconnectedness. As noted by Brunetti et al. (2019) and Das et al. (2022), data confidentiality has often forced researchers to rely on proxies to infer network structures. These include geographical distance, common asset holdings, or volatility spillovers derived from Vector Autoregressions (VAR) (see, e.g., **?**). While these measures capture market sentiment and information transmission, they can diverge significantly from the actual set of bilateral obligations. By exploiting detailed administrative records of interbank loans, we map the 'physical' network of direct financial exposures. This granularity provides a precise identification of the direction and intensity of peer pressure, avoiding the potential measurement errors inherent in market-based approximations.

Finally, we offer a distinct contribution to the econometric literature on efficiency measurement. While the Stochastic Frontier Analysis (SFA) framework remains the standard for benchmarking due to its flexibility (e.g., Kumbhakar et al., 2015), we innovatively extend recent advancements in network-augmented SFA (Hou et al., 2023; Kutlu et al., 2020; Glass et al., 2016; Tran and Tsionas, 2023). Specifically, we adapt the two-step GMM estimation strategy proposed by Hou et al. (2023), originally applied to production functions, to a stochastic cost frontier with fixed effects. This shift is methodologically critical: unlike single-output production models, our cost-based specification is tailored to the multi-output nature of banking, where cost minimization constitutes the primary optimization margin. Furthermore, we replace the standard use of geographic spatial weights with an adjacency matrix derived from actual financial transactions. This dual refinement, shifting from production to cost minimization and from geographic

proxies to 'physical' network measures, provides a more accurate and structurally grounded framework for identifying network dependencies in banking efficiency.

2 Empirical Strategy

We estimate a standard stochastic cost frontier, a widely used framework in banking applications (e.g., Mamonov et al., 2024; Hughes et al., 2019; Tabak et al., 2012; Kumbhakar and Lovell, 2000), and extend the inefficiency term to incorporate network dependence. The cost specification conditions on a conventional set of shifters—outputs, input prices, and quasi-fixed inputs—and includes time-fixed effects. To capture peer interactions, our extension follows the methodology of Hou et al. (2023), modeling a bank's inefficiency as a function of a weighted average of its peers' inefficiencies. The model is estimated using a two-step GMM procedure that identifies the network parameter from the augmented variance–covariance structure. The weights for this interaction are constructed from detailed administrative records on interbank exposures. This setup allows us to explore specifications using both persistent and dynamic network structures, with alternative normalization schemes. This section first presents the econometric model and then details the estimation strategy.

2.1 Econometric Specification

The cost function We specify a translog (TL) stochastic cost frontier for bank $i = 1, \ldots, N$ in time period $t = 1, \ldots, T$:

$$\ln \text{Cost}_{it} = \alpha_t + TL(\boldsymbol{y}_{it}, \boldsymbol{p}_{it}, r_{it}, \boldsymbol{z}_{it}; \boldsymbol{\beta}) + \varepsilon_{it}, \tag{1}$$

where Cost_{it} denotes variable cost; α_t is a time-fixed effect capturing macroeconomic shocks and common shifts in the cost frontier; and $TL(\cdot)$ represents the translog functional form in outputs $\boldsymbol{y}$ (loan categories), input prices $\boldsymbol{p}$ (labor, physical capital, and deposits), quasi-fixed input $\boldsymbol{z}$ (equity capital), and a risk measure r (capital adequacy ratio). The parameter vector $\boldsymbol{\beta}$ collects the technology coefficients. Linear homogeneity in input prices is imposed by normalizing both the dependent variable and the input prices by the price of one input (p_{1it}). Equity capital, given its limited within-bank time variation, also serves as a proxy for bank-specific fixed effects, thereby mitigating unobserved heterogeneity that might otherwise confound the efficiency estimates.

Including a risk measure in the cost function serves two purposes. First, it is standard practice in the banking cost frontier literature: risk-taking affects the cost structure because banks that assume greater risk may incur higher monitoring, provisioning, and funding costs (**?**Hughes et al., 2019; Mamonov et al., 2024). Second, and critically for our setting, the risk control strengthens identification of the network parameter. Because our measure of interconnectedness is derived from interbank debt exposures, banks with higher risk appetites may systematically borrow more in interbank markets, generating a correlation between the adjacency matrix and unobserved cost determinants. In the terminology of Manski (1993),

this constitutes a contextual effect that could confound the estimated endogenous peer effect. Conditioning on risk within the cost function mitigates this sorting concern by absorbing a key dimension along which banks select into network positions.

Interconnectedness and efficiency Following the standard stochastic frontier literature, the error term ε_{it} in equation (1) is decomposed into a symmetric noise term v_{it} and a non-negative inefficiency term u_{it} (Kumbhakar and Lovell, 2000; Kumbhakar et al., 2015). We extend this framework by explicitly modeling network dependence among banks. Specifically, adopting the approach of Hou et al. (2023), we specify the vector of composite errors $\boldsymbol{\varepsilon}_t = (\varepsilon_{1t}, \ldots, \varepsilon_{Nt})'$ as a function of the performance of connected peers, governed by an $N \times N$ adjacency matrix W_t. The structural equation is:

$$\begin{aligned} \boldsymbol{\varepsilon}_t &= \rho W_t \boldsymbol{\varepsilon}_t + \dot{\boldsymbol{\varepsilon}}_t, \\ \dot{\varepsilon}_{it} &= \dot{v}_{it} + \dot{u}_{it}, \end{aligned} \tag{2}$$

where ρ is the network dependence parameter to be estimated. The term $W_t \boldsymbol{\varepsilon}_t$, often expressed component-wise as $\sum_j w_{ijt} \varepsilon_{jt}$ and defined as the endogenous network lag, represents a weighted combination of the composite errors of other banks to which bank i is financially connected. The element w_{ijt} denotes the predetermined weight assigned to the influence of bank j on bank i at time t. This general specification accommodates potentially evolving network structures, with the standard normalization that $w_{iit} = 0$.

A key distinction between our specification and that of Hou et al. (2023) lies in the construction of the adjacency matrix. While Hou et al. assume W to be constant—standard practice in spatial econometrics where intensity is often based on geographic proximity (Elhorst, 2014; LeSage and Pace, 2009; Pace and Barry, 1997)—we leverage detailed administrative data on interbank loan transactions to construct matrices that may vary over time (with the time-invariant matrix being a special case). This dynamic specification represents a significant advance over studies constrained to static interactions (see, e.g., Margaretic et al., 2021). By allowing the network structure to evolve monthly, we capture the changing nature of interbank connections, yielding a more realistic depiction of network effects and potentially enhancing the model's identification. We reserve the detailed discussion of the matrix construction for the Data section; for the current econometric exposition, we rely on the general notation W_t and treat it as a predetermined matrix.

Distributional assumptions and determinants of inefficiency Consistent with the standard stochastic frontier literature (Kumbhakar and Lovell, 2000; Kumbhakar et al., 2015), we assume that the underlying (pre-network) error components are independently distributed. The idiosyncratic noise follows a normal distribution, $\dot{v}_{it} \sim \mathcal{N}(0, \sigma^2_{\dot{v}})$. For the pre-network inefficiency term $\dot{u}_{it}$, we consider two specifications:

Homogeneous inefficiency. Under the baseline specification, the inefficiency term follows a half-normal distribution with a common scale parameter:

$$\dot{u}_{it} \sim \mathcal{N}^+(0, \sigma^2_{\dot{u}}).$$

This imposes that all banks draw inefficiency from the same distribution, so that observed differences in cost performance arise solely from random realizations and the network multiplier.

Heterogeneous inefficiency. Following Hou et al. (2023) (Section 3.3) and Mamonov et al. (2024), we also consider a specification in which the scale of the inefficiency distribution varies across banks as a function of observable characteristics:

$$\dot{u}_{it} \sim \mathcal{N}^{+}\Big(0,\ \sigma^2_{\dot{u}}(\boldsymbol{d}_i;\boldsymbol{\delta})\Big), \quad \text{where} \quad \sigma_{\dot{u}}(\boldsymbol{d}_i;\boldsymbol{\delta}) = \exp\big(\delta_0 + \delta_1 d_i^{\text{own}} + \delta_2 d_i^{\text{seg}}\big). \tag{3}$$

Here d_i^{own} is an indicator for state-owned banks, capturing institutional differences in cost behavior that may arise from public mandates, government guarantees, or distinct operational incentives; and d_i^{seg} is an indicator for banks specializing in the consumer/retail segment, capturing segment-specific cost structures that differ from those of diversified commercial banks. The exponential link function ensures $\sigma_{\dot{u}} > 0$ and allows the scale of inefficiency to vary with bank characteristics while preserving the half-normal distributional assumption. Because our estimation strategy relies on the variance–covariance structure of the composite errors (Hou et al., 2023), incorporating determinants through the variance parameterization is the natural route; it modifies the diagonal of the theoretical covariance matrix, as detailed in Section 2.2.2.

Nesting structure and model variants The specification above nests three models of increasing generality:

M1. *Basic spatial cost frontier.* The cost function excludes the risk regressor (r_{it}) and inefficiency is homogeneous ($\sigma_{\dot{u}}$ is a scalar). The second-stage parameter vector is $\boldsymbol{\theta} = (\rho,\ \sigma^2_{\dot{v}},\ \sigma^2_{\dot{u}})$.

M2. *With risk control.* The risk measure r_{it} enters the translog cost function; inefficiency remains homogeneous. This specification tests whether controlling for risk-taking alters the estimated network dependence.

M3. *With risk and heterogeneous inefficiency.* Risk is included and the inefficiency variance is parameterized as in equation (3), so that $\boldsymbol{\theta} = (\rho,\ \sigma^2_{\dot{v}},\ \boldsymbol{\delta})$. This is the most general specification; it allows both the cost frontier and the inefficiency distribution to differ across bank types.

Estimating all three models allows us to assess robustness and to quantify the incremental contribution of the risk control and of heterogeneous inefficiency to the network dependence estimate $\hat{\rho}$.

2.2 Estimation strategy

Given that a model can be consistently estimated when it is identified, we proceed directly to estimation, rather than addressing identification and consistency issues individually. In particular, for the estimation we follow Hou et al. (2023) and Chanci et al. (2024) and employ a two-step Generalized Method of Moments (GMM) estimation technique for stochastic frontier models involving interactions across units. This GMM framework presents notable advantages over Maximum Likelihood (ML) estimation in this

context. Firstly, unlike the Maximum Like ML method, this approach avoids making full distributional assumptions. Secondly, it circumvents significant numerical optimization complexities associated with ML, such as the requirement for high-dimensional numerical integration within the log-likelihood function or the computational burden arising from a time-variant spatial weighting matrix.[2]

The two-step approach we implement can be summarized as follows: First, we leverage the panel data structure to transform the model and employ a cross-sectional demeaning (or 'between') estimator, thereby avoiding strong initial distributional assumptions. Second, we compute pseudo-residuals from the first-stage estimation. These pseudo-residuals are then used to recover estimates of (in)efficiency, incorporating the adjacency matrix. This step is conducted using GMM, where the moment conditions are based on distributional assumptions for the noise and inefficiency terms. In what follows, we discuss these steps in detail.

2.2.1 First step - Transformation

The model in Equation (1) does not satisfy the standard assumption of classical regression models that the expected value of the error term is zero. Specifically, when u_{it} follows the structure defined in Equation (2), the composite error $\varepsilon_{it} = v_{it} + u_{it}$ has a non-zero expectation: $\mathbb{E}[\varepsilon_{it}] = \mathbb{E}[v_{it} + u_{it}] = \mathbb{E}[u_{it}]$, which represents the mean inefficiency level.

Nonetheless, although the error mean is non-zero, it is possible to rewrite the model by absorbing this term into a time-specific intercept. The model from Equation (1) then becomes:

$$\ln \text{Cost}_{it} = \alpha_t^* + TL(\boldsymbol{y}_{it}, \boldsymbol{p}_{it}, r_{it}, \boldsymbol{z}_{it}; \boldsymbol{\beta}^*) + \varepsilon_{it}^*, \tag{4}$$

where the parameter vector $\boldsymbol{\beta}^*$ now excludes the original intercept β_0; the new time-specific intercept is $\alpha_t^* = \beta_0 + \alpha_t + \mathbb{E}[u_{it}]$; and the transformed error term is $\varepsilon_{it}^* = v_{it} + u_{it} - \mathbb{E}[u_{it}]$. Therefore, by construction, $\mathbb{E}[\varepsilon_{it}^*] = 0$, and the resulting model belongs to the family of panel data models (i.e., a panel cost function featuring time-specific effects, where time-invariant individual heterogeneity is primarily accounted for by including quasi-fixed inputs, rather than via separate individual-specific intercepts).

Considering that the fixed effects are nuisance parameters in our case, and given that the time dimension, T, in our dataset is large, we rely on a within-time transformation rather than using time dummy variables for the time fixed effects. Hence, we first employ a transformation approach to eliminate the time effects in equation (4). Let $Q = (I_N - (1/N)\iota_N \iota_N')$ be the $N \times N$ matrix used to compute the demeaned variables in the within-time transformation, as established in the panel data literature (e.g., Baltagi, 2021), where ι_N is an $N \times 1$ vector of ones. In this way, one can remove the time effects α_t^* using Q. Specifically, let us denote a vector variable with a tilde as the result of pre-multiplying the vector by Q. For instance, $\widetilde{\boldsymbol{z}}_t$ is an $N \times 1$ vector, resulting from $Q\boldsymbol{z}_t$, where $\boldsymbol{z}_t = (z_{1t}, ..., z_{Nt})'$.[3] Applying this transformation to Equation (4) eliminates the time-specific effect α_t^*. Thus, since the translog function

[2] If W_t enters the likelihood function via the error structure (e.g., through terms involving $(I - \rho W_t)^{-1}$ that must be computed for each time period t), it substantially complicates the ML optimization compared to the moment-based GMM approach used here.

[3] This is also equivalent to $\widetilde{z}_{it} = (z_{it} - z_{\cdot t})$, where $z_{\cdot t} = N^{-1} \sum_i z_{it}$.

$TL(\cdot)$ is linear in the parameters $\boldsymbol{\beta}^*$, and the Q transformation is a linear operator, the resulting model remains linear in $\boldsymbol{\beta}^*$:

$$\widetilde{\ln \text{Cost}}_t = \sum_k \beta_k^* \widetilde{X}_{kt} + \widetilde{\varepsilon}_t^* \tag{5}$$

where the regressors $\widetilde{X}_{kt}$ are the transformed versions (QX_{kt}) of each vector X_{kt} representing a term required by the translog specification (e.g., vectors of element-wise logs like $\ln y_{it}$, squares like $(\ln y_{it})^2$, or cross-products like $\ln y_{it} \ln p_{it}$), constructed from the original data vectors $(\boldsymbol{y}_t, \boldsymbol{p}_t, r_t, \boldsymbol{z}_t)$. As the transformed error $\widetilde{\varepsilon}_t^* = Q\varepsilon_t^*$ retains the zero-mean property (since $\mathbb{E}[\varepsilon_t^*] = \mathbf{0}$), Equation (5) satisfies the requirements for consistent estimation of $\boldsymbol{\beta}^*$ via Ordinary Least Squares (OLS). Therefore, applying OLS yields the first-stage estimates $\hat{\boldsymbol{\beta}}^*$ of $\boldsymbol{\beta}^*$ without using distributional assumptions on ν_{it} and u_{it}, avoiding computational challenges associated with the ML method.

2.2.2 Second step: GMM estimation

The second stage of our estimation procedure utilizes the parameter estimates $\hat{\boldsymbol{\beta}}^*$ obtained from the first step. Recalling Equation (1):

$$\ln \text{Cost}_{it} - TL(\boldsymbol{y}_{it}, \boldsymbol{p}_{it}, r_{it}, \boldsymbol{z}_{it}; \boldsymbol{\beta}^*) = \beta_0 + \alpha_t + \nu_{it} + u_{it}$$

We construct the pseudo-residuals, denoted by e_{it}, using the first-step estimates $\hat{\boldsymbol{\beta}}^*$:

$$e_{it} = \ln \text{Cost}_{it} - TL(\boldsymbol{y}_{it}, \boldsymbol{p}_{it}, r_{it}, \boldsymbol{z}_{it}; \hat{\boldsymbol{\beta}}^*) \tag{6}$$

These pseudo-residuals approximate the composite error term plus the intercept and time effects, $e_{it} \approx \beta_0 + \alpha_t + \nu_{it} + u_{it}$. As established earlier, we can decompose the right-side of this expression into a time-specific mean component $\alpha_t^* = (\beta_0 + \alpha_t + \mathbb{E}[u_{it}])$ and a zero-mean error component $\varepsilon_{it}^* = (\nu_{it} + u_{it} - \mathbb{E}[u_{it}])$. Thus, $e_{it} \approx \alpha_t^* + \varepsilon_{it}^*$. Since by construction $\mathbb{E}[\varepsilon_{it}^*] = 0$, the time-specific mean component α_t^* can be consistently estimated by the cross-sectional average of the pseudo-residuals for each period t: $\hat{\alpha}_t^* = N^{-1} \sum_i e_{it}$. In what follows, we use this estimate $\hat{\alpha}_t^*$ to obtain residuals suitable for estimating the (in)efficiency structure. In particular, we define the adjusted residuals $\bar{e}_{it}$ by removing this estimated time-specific mean: $\bar{e}_{it} = e_{it} - \hat{\alpha}_t^*$. Thus, substituting the approximations yields the central equation for the second stage:

$$\bar{e}_{it} = \nu_{it} + u_{it} - \mathbb{E}[u_{it}] \tag{7}$$

Equation (7) represents a Stochastic Frontier (SF) model structure based on these adjusted residuals $\bar{e}_{it}$. Here, ν_{it} is the two-sided random noise and $(u_{it} - \mathbb{E}[u_{it}])$ is the (mean-shifted) one-sided inefficiency term. Therefore, the second-stage GMM procedure can use distributional assumptions on the underlying components ν_{it} and u_{it} (particularly their network-independent counterparts $\dot{\nu}_{it}, \dot{u}_{it}$) to formulate moment conditions for estimating the network dependence parameter ρ, the variance parameters ($\sigma_{\dot{\nu}}^2$ and either $\sigma_{\dot{u}}^2$ or $\boldsymbol{\delta}$), and the mean inefficiency $\mathbb{E}[u_{it}]$.

As mentioned, given that our model specification in Equation (2) incorporates dependency in banking performance via the time-variant weights matrix W_t, the ML estimation for the becomes complex. Thus, we closely follow the estimation approach proposed by Hou et al. (2023) (henceforth, HZK). They propose GMM estimation for a semiparametric stochastic frontier model incorporating spatial dependence. Although their model features functional coefficients while our specification uses constant parameters (including fixed effects), the dependence structure applied to the second-stage error components is analogous, allowing the adaptation of their GMM procedure.

In short, the GMM estimation identifies the network dependence parameter ρ and the variance parameters associated with the underlying structurally independent noise ($\dot{\nu}_{it}$) and inefficiency ($\dot{u}_{it}$) components. This relies on exploiting moment conditions derived from the distributional assumptions on $\dot{\nu}_{it}$ and $\dot{u}_{it}$. In particular, let $S(\rho, W_t) = (I_N - \rho W_t)^{-1}$. Since $\boldsymbol{\varepsilon}_t = S(\rho, W_t)(\dot{\boldsymbol{\nu}}_t + \dot{\boldsymbol{u}}_t)$ and the pre-network components are independent, the second-moment condition based on the variance-covariance structure is:

$$\mathbb{V}(\boldsymbol{\varepsilon}_t) = S(\rho, W_t)\left[\sigma^2_{\dot{\nu}} I_N + \left(1 - \frac{2}{\pi}\right)\Sigma_{\dot{u},t}\right](S(\rho, W_t))^\top \tag{8}$$

where $\Sigma_{\dot{u},t}$ encodes the inefficiency variance structure. Under the homogeneous specification (M1, M2), $\Sigma_{\dot{u},t} = \sigma^2_{\dot{u}} I_N$, reducing the bracketed term to the scalar $[\sigma^2_{\dot{\nu}} + (1 - 2/\pi)\sigma^2_{\dot{u}}]I_N$. Under the heterogeneous specification (M3), $\Sigma_{\dot{u},t} = \text{Diag}\big(\sigma^2_{\dot{u}}(\boldsymbol{d}_1; \boldsymbol{\delta}), \ldots, \sigma^2_{\dot{u}}(\boldsymbol{d}_N; \boldsymbol{\delta})\big)$, where each diagonal entry is determined by the bank's characteristics through the exponential link in equation (3).

The sample counterpart for the $N \times N$ theoretical variance-covariance matrix $\mathbb{V}(\boldsymbol{\varepsilon}_t)$ is constructed for each time period t using the adjusted residuals $\bar{\boldsymbol{e}}_t = (\bar{e}_{1t}, \ldots, \bar{e}_{Nt})^\top$ from Equation (7). Thus, as $\mathbb{E}[\bar{e}_{it}] = 0$, the time-specific sample variance-covariance matrix is calculated as $\hat{V}_t = \bar{\boldsymbol{e}}_t \bar{\boldsymbol{e}}_t^\top$. According to HZK, leveraging the principle of minimum distance estimation, the unknown parameter vector $\boldsymbol{\theta}$—equal to $(\rho, \sigma^2_{\dot{\nu}}, \sigma^2_{\dot{u}})$ in the homogeneous case or $(\rho, \sigma^2_{\dot{\nu}}, \boldsymbol{\delta})$ in the heterogeneous case—can be estimated by minimizing the distance between these sample covariance matrices $\hat{V}_t$ and their theoretical counterparts $\mathbb{V}(\boldsymbol{\varepsilon}_t; \boldsymbol{\theta})$ over time. Specifically, the parameters are chosen to minimize the GMM objective function:

$$\min_{\boldsymbol{\theta}} Q(\boldsymbol{\theta}) = \min_{\boldsymbol{\theta}} \sum_{t=1}^{T} \left\| \hat{V}_t - \mathbb{V}(\boldsymbol{\varepsilon}_t; \boldsymbol{\theta}) \right\|_F^2 \tag{9}$$

where $\|\cdot\|_F$ denotes the Frobenius norm, and $\mathbb{V}(\boldsymbol{\varepsilon}_t; \boldsymbol{\theta})$ is the theoretical variance-covariance matrix defined in Equation (8).

Furthermore, considering that practical optimization of $Q(\boldsymbol{\theta})$ may encounter challenges such as multiple local minima or irregular objective function surfaces, we adopt a improved deviation from HZK regarding the numerical computation of $\boldsymbol{\theta}$. Specifically, we enhance numerical stability and efficiency by noting that the estimation must respect the constraint $|\rho| < 1$, associated with the invertibility of the $S(\rho, W_t)$ term. We thus implement a grid search strategy, widely used in the spatial econometrics literature (see, e.g., Elhorst, 2014, 2010; Pace and Barry, 1997). This involves a grid search over the permissible range $\rho \in (-1, 1)$. For each candidate value ρ_j from the grid, the GMM objective function

is minimized with respect to the remaining parameters—$(\sigma^2_{\dot{v}}, \sigma^2_{\dot{u}})$ in the homogeneous case, or $(\sigma^2_{\dot{v}}, \boldsymbol{\delta})$ in the heterogeneous case—to obtain conditional estimates. The optimal estimate $\hat{\rho}$ is then selected as the value ρ_j that yields the global minimum of the GMM objective function in Equation (9) across all tested grid points, along with its corresponding conditional estimates.[4]

2.2.3 Post-Estimation Calculations

Once the GMM estimation yields consistent estimates of $\hat{\rho}$, $\hat{\sigma}^2_{\dot{v}}$, and the inefficiency parameters ($\hat{\sigma}^2_{\dot{u}}$ or $\hat{\boldsymbol{\delta}}$), further quantities of interest can be derived.

First, we estimate the mean inefficiency component $\mathbb{E}[\boldsymbol{u}_t]$. Under the homogeneous specification, $\dot{u}_{it}$ follows a half-normal distribution with common scale, so $\mathbb{E}[\dot{\boldsymbol{u}}_t] = \sqrt{2/\pi}\,\hat{\sigma}_{\dot{u}}\,\iota_N$, and the estimate incorporating the network multiplier is:

$$\hat{\mathbb{E}}[\boldsymbol{u}_t] = \sqrt{\frac{2}{\pi}}\hat{\sigma}_{\dot{u}}\, S(\hat{\rho}, W_t)\iota_N$$

where ι_N is an $N \times 1$ vector of ones. Since in our application the weights matrix W_t is row-normalized for each t, $S(\hat{\rho}, W_t)\iota_N$ is a constant vector, and mean inefficiency is identical across banks within each period. Under the heterogeneous specification (M3), $\hat{\sigma}_{\dot{u}}$ is replaced by the bank-specific vector $\hat{\boldsymbol{\sigma}}_{\dot{u}} = (\hat{\sigma}_{\dot{u}}(\boldsymbol{d}_1; \hat{\boldsymbol{\delta}}), \ldots, \hat{\sigma}_{\dot{u}}(\boldsymbol{d}_N; \hat{\boldsymbol{\delta}}))'$, so that:

$$\hat{\mathbb{E}}[\boldsymbol{u}_t] = \sqrt{\frac{2}{\pi}}\, S(\hat{\rho}, W_t)\, \hat{\boldsymbol{\sigma}}_{\dot{u}}$$

and mean inefficiency varies across banks even within the same period.

Second, we recover estimates of the combined constant and time fixed effects, which will be later used in the computation of the standard errors. Recalling the estimated time-specific component $\hat{\alpha}^*_t = \bar{e}_t$, which consistently estimates $\alpha^*_t = \beta_0 + \alpha_t + \mu$, one can compute: $\widehat{(\beta_0 + \alpha_t)} = \hat{\alpha}^*_t - \hat{\mathbb{E}}[u_{it}]$.[5]

Third, following HZK's adaptation of Jondrow et al. (1982) (JLMS), we predict the bank-specific inefficiency component. This term is defined by the conditional expectation of the underlying network-independent $\dot{u}_{it}$ given the underlying network-independent composite error $\dot{\varepsilon}_{it}$:

$$\dot{\mu}_{it} = \mathbb{E}[\dot{u}_{it}|\dot{\varepsilon}_{it}] = \mu^*_{it} + \sigma_* \frac{\phi(-\mu^*_{it}/\sigma_*)}{1 - \Phi(-\mu^*_{it}/\sigma_*)} \tag{10}$$

where $\mu^*_{it} = \dot{\varepsilon}_{it}\sigma^2_{\dot{u},i}/(\sigma^2_{\dot{u},i} + \sigma^2_{\dot{v}})$ and $\sigma_{*,i} = \sqrt{\sigma^2_{\dot{u},i}\sigma^2_{\dot{v}}/(\sigma^2_{\dot{u},i} + \sigma^2_{\dot{v}})}$, using the estimated variance parameters. In the homogeneous case, $\sigma^2_{\dot{u},i} = \sigma^2_{\dot{u}}$ for all i; in the heterogeneous case, $\sigma^2_{\dot{u},i} = \sigma^2_{\dot{u}}(\boldsymbol{d}_i; \boldsymbol{\delta})$

[4] To efficiently locate the minimum, we first employ a coarser grid for ρ (e.g., using 0.1 increments) to find an initial optimum, followed by a finer grid search (e.g., using 0.001 increments) in the neighborhood of that initial value. This vectorized grid search approach, potentially combined with parallel computing techniques, speeds up the estimation within the GMM framework.

[5] Separating the overall constant β_0 from the individual time effects α_t would require an additional normalization constraint (e.g., $\sum_t \alpha_t = 0$), which is not pursued here.

varies by bank.

The unobserved $\dot{\varepsilon}_{it}$ required for Equation (10) is obtained via the relationship $\dot{\boldsymbol{\varepsilon}}_t = (I_N - \rho W_t)\boldsymbol{\varepsilon}_t$. Thus, we approximate the unobserved vector $\boldsymbol{\varepsilon}_t = \boldsymbol{\nu}_t + \boldsymbol{u}_t$ by combining the adjusted residuals with the estimated mean inefficiency according to Equation (7), $\hat{\boldsymbol{\varepsilon}}_t \approx \bar{\boldsymbol{e}}_t + \hat{\mathbb{E}}[u_t]$. Subsequently, we compute the estimate $\hat{\dot{\boldsymbol{\varepsilon}}}_t$. The i-th element of this vector, $\hat{\dot{\varepsilon}}_{it}$, is then plugged into Equation (10) to obtain the conditional estimate $\hat{\dot{\mu}}_{it} = \widehat{\mathbb{E}[\dot{u}_{it}|\dot{\varepsilon}_{it}]}$. The final prediction of the actual inefficiency term is constructed from these estimates using the specific network transformation, $\text{Inefficiency}_t = \hat{\boldsymbol{\mu}}_t = S(\hat{\rho}, W_t) * \hat{\dot{\boldsymbol{\mu}}}_t$, as detailed in HZK.

Finally, we conduct a decomposition of (in)efficiency estimates that offers valuable insights into the relative importance of internal factors versus interconnectedness in determining observed banking performance. Specifically, considering that total bank inefficiency is related to underlying network-independent components via $S(\hat{\rho}, W_t)\hat{\dot{\boldsymbol{\mu}}}_t$, we can decompose the estimated total cost inefficiency into effects originating from the bank's own underlying inefficiency component and effects spilling over from other banks through the network (e.g., peer effects). Let the total inefficiency for bank i at time t be $\sum_{j=1}^{N} s_{ij}\hat{\dot{\mu}}_{jt}$, where s_{ij} is an element of $S(\hat{\rho}, W_t)$. This sum can thus be separated into two terms as follows:

$$\text{Total Inefficiency}_{it} \equiv s_{ii}\hat{\dot{\mu}}_{it} + \sum_{j \neq i} s_{ij}\hat{\dot{\mu}}_{jt} \equiv \text{Direct Effect}_{it} + \text{Indirect (Network) Effect}_{it}$$

Thus, the Direct Effect isolates the impact of a bank's own underlying inefficiency, scaled by the feedback effect s_{ii} from the diagonal of the multiplier matrix S. The Indirect Effect, on the other hand, captures the net influence of all other banks' underlying inefficiencies propagated through the network via the off-diagonal elements (s_{ij}) of S.

2.2.4 Computation of Standard Errors via Wild Bootstrap

Given the multi-step nature of our GMM estimation procedure for the stochastic cost frontier with interconnectedness, deriving analytical standard errors is complex. Therefore, we employ a wild bootstrap approach to assess the sampling variability of the estimated parameters ($\hat{\rho}$, $\hat{\sigma}_{\dot{v}}$, and $\hat{\sigma}_{\dot{u}}$. This method is well-suited for models with complex error structures and potential heteroskedasticity, and its applicability to spatial models has been already discussed (see, e.g., HZK for simulation results in a related GMM framework, and Gonçalves and Perron, 2020, for wild bootstrap with cross-sectional dependence).

Our wild bootstrap procedure is adapted to the specific structure of our model, where the composite error ε_{it} is transformed into an underlying, network-independent structural error $\dot{\varepsilon}_{it}$ via the relation $\dot{\boldsymbol{\varepsilon}}_t = (I_N - \hat{\rho} W_t)\boldsymbol{\varepsilon}_t$. The core idea is to resample these estimated network-independent residuals $\hat{\dot{\varepsilon}}_{it}$. In particular, for each bootstrap replication $b = 1, \ldots, B$, the procedure is as follows:

1. **Generate bootstrap multipliers:** We generate a vector of bootstrap multipliers $\boldsymbol{\xi}^{(b)}$ of dimension $NT \times 1$ (where N is the number of banks in period t, and NT is the total number of observations).

These multipliers are drawn independently from the Mammen (1993) two-point distribution:

$$\xi_{it}^{(b)} = \begin{cases} -(\sqrt{5}-1)/2 & \text{with probability } p = (\sqrt{5}+1)/(2\sqrt{5}) \\ (\sqrt{5}+1)/2 & \text{with probability } 1-p \end{cases}$$

The estimated underlying structural residuals $\hat{\varepsilon}_{it}$ are then perturbed to create bootstrapped structural residuals: $\varepsilon_{it}^{(b)} = \hat{\varepsilon}_{it} \cdot \xi_{it}^{(b)}$.

2. **Construct bootstrapped dependent variable:** Using the parameters from the initial estimation ($\widehat{\beta_0 + \alpha_t}$, $\hat{\boldsymbol{\beta}}^*$, and $\hat{\rho}$), we construct the bootstrapped log-cost variable, $\ln Cost_{it}^{(b)}$:

$$\ln \boldsymbol{Cost}_t^{(b)} = (\widehat{\beta_0 + \alpha_t})\boldsymbol{\iota}_{N_t} + TL(\boldsymbol{y}_t, \boldsymbol{p}_t, r_t, \boldsymbol{z}_t; \hat{\boldsymbol{\beta}}^*) + (I_N - \hat{\rho} W_t)^{-1} \hat{\boldsymbol{\varepsilon}}_t^{(b)}$$

3. **Re-estimate parameters:** The full two-step estimation procedure, as outlined in Section 2, is applied to the dataset with $\ln Cost_{it}^{(b)}$ as the dependent variable.

This entire process is repeated B times. The standard error for each element of $\boldsymbol{\theta}$—i.e., ρ, $\sigma_{\dot{\nu}}$, and either $\sigma_{\dot{u}}$ (homogeneous models) or the vector $\boldsymbol{\delta}$ (heterogeneous model)—is then calculated as the empirical standard deviation of its B bootstrapped estimates.

3 Data

Our research utilizes a granular dataset combining detailed records from the Chilean interbank lending market with bank-specific balance sheet characteristics. Access to this confidential administrative data, provided by the Chilean Financial Market Commission (CMF), enables a precise analysis of banking interconnectedness and its impact on performance. As previously noted, our dataset addresses common limitations identified in the literature, where researchers often lack direct measures of micro-level linkages and instead rely on aggregated data or proxy approximations.[6]

Although Chile is a relatively smaller economy compared to global financial hubs such as the United States or Europe, its banking system provides an ideal context for investigating the role of interconnectedness in bank performance for several reasons. First, despite comprising a limited number of institutions—our sample includes 20 banks, virtually representing the entire sector—the Chilean banking system is mature, relatively concentrated, and plays a substantial role proportional to the overall economy (Margaretic et al., 2021). Such characteristic enhances the visibility and measurability of network dynamics and their effects on individual institutions. Second, and crucially for our empirical strategy, Chile offers exceptional access to detailed administrative datasets. These comprehensive datasets enable the accurate

[6]Due to confidentiality concerns, initial model development and preliminary analyses were conducted using anonymized data that preserves essential statistical properties while safeguarding bank identities. Final computational analyses using the complete, non-anonymized dataset were executed exclusively by authorized CMF personnel to ensure data security and confidentiality. External researchers, therefore, did not have direct access to sensitive identifying information.

construction of real interbank lending networks using daily transaction records and detailed monthly balance sheets over an extended period (e.g., 2008–2020 in our full dataset). Thus, the high-frequency monthly data introduces a rich temporal dimension (T), resulting in a substantial and informative panel dataset. This dataset allows for robust analysis of dynamic network effects and efficiency, offering insights often unavailable from larger systems with less comprehensive data.

Information on interbank exposures is obtained from regulatory reports submitted by all active banks in Chile to the CMF. Specifically, we use Form C-18, titled Daily Balances of Obligations with Other Domestic Banks (*Saldos Diarios de Obligaciones con Otros Bancos del País*, in Spanish), which details all daily bilateral exposures between institutions. These reports are comprehensive, categorizing obligations across a range of financial instruments, including current accounts, other sight obligations, repurchase agreements, term deposits, and financial derivative contracts. Furthermore, the data differentiates exposures by residual maturity using three specific categories: sight obligations, obligations with maturity up to one year, and obligations with maturity over one year. The data also classifies each obligation by its currency of payment, distinguishing between non-indexed Chilean pesos, indexed domestic currency, and foreign currency.

For the main round of results presented in this paper, we construct the weights matrix (W_t) using a comprehensive measure of total interbank obligations. The weight of the connection between any two banks is defined as the sum of all reported financial instruments (including term deposits, repurchase agreements, and derivatives) across all available maturity categories (sight, up to one year, and over one year). Consistent with the C-18 reporting structure, our network is directed, with edges running from the borrower (the reporting institution) to the lender (the creditor institution). After aggregating the data to a monthly frequency, we apply a row-normalization to the resulting time-varying adjacency matrices. This is a standard and effective way to measure the relative importance of each lender to a specific borrower, as the normalized weight represents a lender's share of a given borrower's total obligations.

While this comprehensive matrix based on total obligations forms the basis of our core results, we leverage the granularity and depth of our administrative data to explore alternative specifications of W_t in a subsequent section. These alternative settings—which consider different combinations of financial instruments and maturities, alternative normalization methods, and the reverse lender-to-borrower direction—serve as both robustness checks and a method for analyzing potential transmission channels. The ability to construct and test these varied network specifications using direct, dynamic, and detailed transaction data provides a uniquely rich framework for analyzing the multifaceted role of interconnectedness.

Complementing the interbank exposure data, we employ comprehensive bank-specific financial information from monthly balance sheets submitted to the CMF (Form MB-2). These reports provide detailed information on each bank's financial position, operational activities, and risk profiles.

The final dataset is constructed as a monthly panel that combines bilateral interbank exposure data—used to define the network structures (W_t)—with detailed bank-specific balance sheet variables for the full set of the 20 most important banks operating in Chile. This rich, panel-structured dataset allows for robust empirical analysis of banking performance through advanced econometric techniques designed for panel and network data, while effectively controlling for bank heterogeneity and time-specific effects.

Note: Although our full dataset spans from 2008 to 2020, covering virtually the entire Chilean interbank market, this preliminary analysis (working paper) utilizes data for the period from January 2016 to December 2017. To ensure comparability over time, all nominal variables have been deflated using the Chilean Consumer Price Index (CPI), with 2018 as the base year.

3.1 Variable Definitions for the Cost Function Estimation

Following the standard intermediation approach in the banking literature (e.g., Sealey Jr and Lindley, 1977; Malikov et al., 2015), we define bank outputs, inputs, and input prices based on the balance sheet information derived from the CMF data.

Table 1: Variable Definitions and Statistics

Variable	Description	Mean	Min.	Max.	Std. Dev.
Outputs (y):					
y_1	Commercial loans	7447258	0	127254619	16671362
y_2	Real estate loans (Mortgages)	3333666	0	68397203	8015098
y_3	Consumer loans	1597754	0	27530158	3710158
y_4	Securities and other investments	1663284	0	55740117	4220972
Inputs (x) and their Prices (p):					
x_1	Labor	3312	20	11521	3681
x_2	Physical capital (Fixed assets)	113510	0	1466479	256413
x_3	Deposits and other borrowed funds	10349058	0	180746605	23321380
p_1	Labor price	-108972	-2853901	0	277452
p_2	Physical capital price	-5665	-147212	0	14416
p_3	Price of funds	-242834	-6183112	30306	615377
Quasi-fixed Input:					
z_1	Equity capital	1447764	0	24272083	3195097
Cost:					
C	Total variable operating cost	-377345	-9790558	0	949620

Notes: 1. The table reports the variables employed in the translog cost function. 2. Labor refers to the total number of workers. 3. All monetary values, except for Labor, are expressed in thousands of Chilean pesos. 4. Real values were computed using the 2018 CPI from the Central Bank of Chile. 5. Std. Dev. in the last column denotes the standard deviation.

We specify four output categories representing key earning assets: commercial loans, real estate loans, consumer loans, and securities and other investments. All outputs are measured in real Chilean Pesos of 2018.

Variable inputs include labor, measured by total personnel expenses and number of employees; physical capital, represented by the book value of fixed and leased assets; and borrowed funds (including deposits). Input prices are computed by dividing the respective expenses by the input quantities.

We include equity capital as a quasi-fixed input to control for bank heterogeneity and scale. Total variable operating cost is constructed as the sum of interest expenses, commissions, personnel expenses, and selected administrative expenses, excluding depreciation to avoid double counting with the capital input price.

4 Results

4.1 The Cost Function and Network Dependence

As previously discussed, while the first-stage allows us to obtain the central parameters in the empirical cost function, β, the second-stage GMM estimation enables the quantification of the average degree of interdependence in bank cost performance deviations, through the parameter ρ, and the key standard deviations in the Cost Function. Given the large numbers of terms in the vector, and as it is common in the literature, for the estimated trans-log cost function we mainly report key associated results, such as the standard deviations that allow the differentiation of the two components in the composited residual and the computation of the estimates of cost efficiency.

Our estimation, reported in Table 2, yields $\hat{\rho} = -0.542$, which is statistically significant. The negative estimate indicates a negative correlation in inefficiency deviations among interconnected banks. In other words, a bank linked to peers exhibiting higher-than-average inefficiency tends to show lower adjusted inefficiency itself. This pattern suggests that banks connected to less efficient neighbors, on average, operate more efficiently relative to their own expected cost levels. Such a finding is consistent with the notion that banks may face competitive pressures or engage in negative benchmarking—improving their efficiency by observing and avoiding the mistakes made by underperforming peers. These dynamics point to meaningful network effects, potentially driven by strategic responses to peer underperformance or by negative learning mechanisms, wherein banks adapt their strategies after witnessing adverse outcomes among their counterparts.

In the following subsections we present relevant post-estimation results, including bank-level inefficiency scores and a decomposition of the relative contributions of direct and network effects to overall performance. We conclude by exploring potential mechanisms underlying the observed negative network dependence.

Table 2: Results for the central parameters

	M1	**M2**	**M3**
	Baseline	With Risk	Determinants
Panel A. Interconnectedness parameter			
ρ	**-0.095** ***	**-0.066** **	**-0.066** ***
	(0.033)	(0.032)	(0.023)
Panel B. Cost frontier main parameters			
σ_v	0.019	0.017	0.115 ***
	(0.012)	(0.015)	(0.003)
σ_u	0.2 ***	0.189 ***	
	(0.007)	(0.004)	
Panel C. Inefficiency determinants (M3)			
δ_0 (Constant)			-9.94 ***
			(0.573)
δ_1 (Ownership)			-16.41 ***
			(0.458)
δ_2 (Segment)			-12.222 ***
			(0.308)
Controls in the Translog Cost Function	Yes	Yes	Yes
Time fixed effects	Yes	Yes	Yes
Observations	1783	1783	1783

Notes: 1. The table reports the central results for the parameters in equations (1) and (2). M1 is the baseline spatial cost frontier; M2 adds a capital adequacy ratio as risk regressor; M3 replaces the scalar σ_u with inefficiency determinants (δ vector). The 'Controls in the Translog Cost Function' row indicates the inclusion of all first-order, second-order (squared), and interaction terms for outputs, input prices, and quasi-fixed inputs as specified in the translog cost function $TL(\boldsymbol{y}_{it}, \boldsymbol{p}_{it}, \boldsymbol{z}_{it}; \boldsymbol{\beta}^*)$ in equation (1). 2. Data: Chilean banking system (2010m1–2018m1). 3. Standard errors (in parentheses) computed via wild bootstrap. 4. *** significant at 1%; ** 5%; * 10%.

4.2 Baseline Banking Performance: Cost Efficiency Levels

We first briefly present the baseline estimates of banking cost efficiency derived from our stochastic cost frontier model. This initial overview serves to characterize the general performance landscape of the Chilean banking industry and to verify that our estimates, despite the econometric novelties introduced, align broadly with findings from previous research on this sector.

Figure 1 illustrates the empirical distribution and temporal evolution of the technical efficiency scores,

calculated as $TE_{it} = \exp(-\hat{\mu}_{it})$, where $\hat{\mu}_{it}$ is the estimated cost inefficiency presented in subsection 2.2.3. Panel (a) of the figure shows the kernel density estimate of these scores, and Panel (b) presents a time series of monthly boxplots illustrating their distribution. The results suggest that the Chilean banking system generally operates at high levels of cost efficiency. The scores are predominantly concentrated towards the upper end of the scale, with a central tendency suggesting typical efficiency levels around 90% (i.e., a TE score of approximately 0.9). While exhibiting some cross-sectional heterogeneity, these efficiency levels are relatively stable over the observed period. These initial findings are consistent with other empirical assessments of the Chilean banking industry (e.g., Cobas et al., 2024), which supports our model's baseline characterization of bank performance as a necessary preliminary step before analyzing network effects.

Figure 1: Technical Efficiency Scores

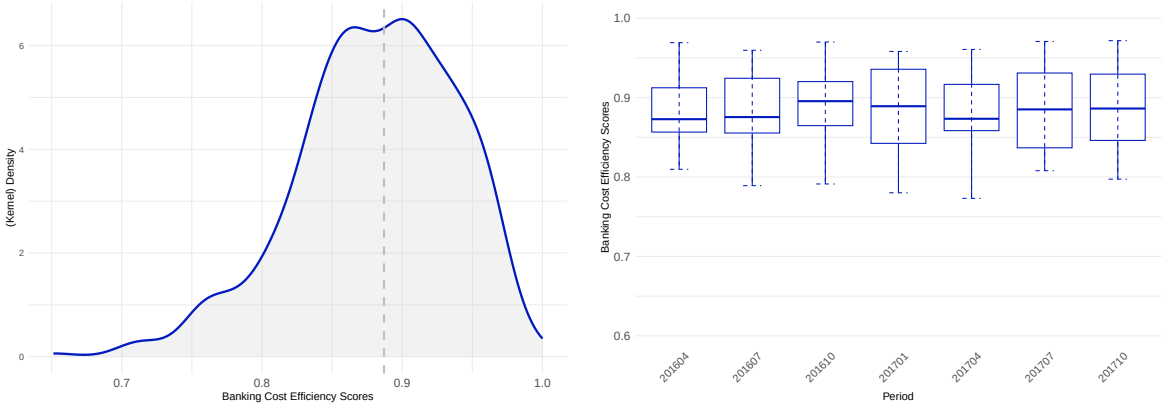

(a) Distribution (b) Temporal Evolution

Notes: The figure has two panels and presents the Distribution and Temporal Evolution of Bank Technical Efficiency Scores (2016m01–2017m12). Panel (a) displays the kernel density estimate of technical efficiency scores pooled across all banks and months in the sample period. Panel (b) presents a time series of monthly boxplots, illustrating the distribution of these scores for selected months. Technical efficiency scores (TE_{it}) are calculated as the exponential of the negative estimated cost inefficiency term, i.e., $TE_{it} = \exp(-\hat{\mu}_{it})$.

4.3 Interconnectedness and Banking Performance

The statistically significant network dependence parameter ($\hat{\rho}$) presented in Table 2 provides initial empirical evidence for the role of interbank interconnectedness in shaping banking performance within our dataset, an overall result that aligns with previous findings on peer effects (Margaretic et al., 2021). A key novelty of our econometric approach, however, is its ability to leverage this estimated parameter and the weights matrix (W_t) to quantify the importance of such interconnectedness. This is achieved by decomposing the total estimated cost inefficiency into a Direct Effect component (representing Idiosyncratic

Inefficiency, $s_{ii}\hat{\mu}_{it}$) and an Indirect (Network) Effect component ($\sum_{j\neq i} s_{ij}\hat{\mu}_{jt}$), as detailed in Subsection 2.2.3.

We find that the Indirect (Network) Effect component is, on average, negative. This finding is directly associated with our negative estimate for the network dependence parameter ($\hat{\rho} = -0.542$), given that the underlying, network-independent inefficiency estimates ($\hat{\mu}_{it}$ from Equation 10) and the elements of the weights matrix (W_t) are non-negative. Specifically, a negative $\hat{\rho}$ introduces negative dependencies within the network multiplier matrix $S(\hat{\rho}, W_t)$. Consequently, for a bank connected to peers with higher underlying inefficiency, the network effect tends to yield a net reduction in that bank's total cost inefficiency, relative to its own Direct Effect component.

Figure 2 visually presents this efficiency-enhancing role of network interactions in the Chilean interbank market. The figure presents kernel density estimates comparing the distributions of the Idiosyncratic Inefficiency component (Direct Effect, red line) and the final Total Inefficiency estimate (blue line) across all bank-period observations. A clear leftward shift is observed for the distribution of Total Inefficiency relative to that of the Idiosyncratic Inefficiency. This displacement means that the predominantly negative Indirect (Network) Effects lead to Total Inefficiency levels that are, on average, lower than what would be implied by banks' idiosyncratic components alone. Thus, the interconnections within the interbank lending market, as captured by our model, appear to play a significant role in improving overall cost efficiency in the sector.

Figure 2: Kernel Density of the Direct and Total Effects

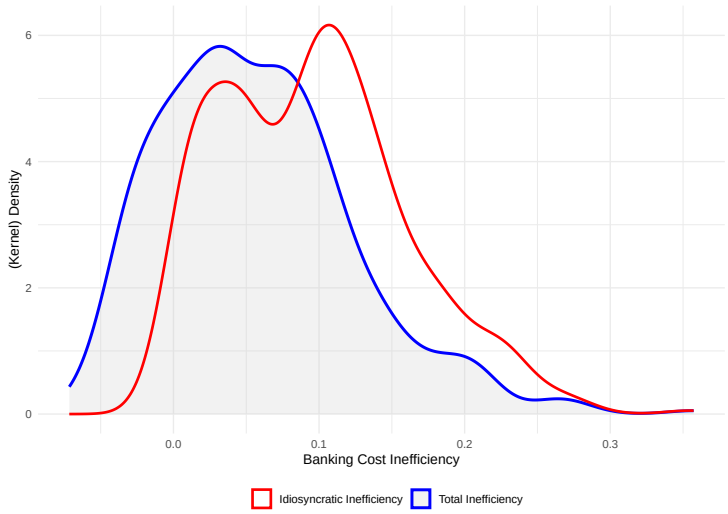

Notes: The figure contains two kernel density plots. These depict estimates of the Direct or Idiosyncratic component of cost inefficiency (red line) and the Total component (blue line), with data pooled across all banks and months in the sample period.

To further quantify the economic significance of the network effects—suggested by the leftward shift in the inefficiency distributions shown in Figure 2—we introduce an intuitive metric termed "Efficiency

Gain." This measure captures the percentage reduction in a bank's cost inefficiency attributable to network interactions, relative to its Direct (Idiosyncratic) Effect. Formally, it is computed as $(1 - \text{Total Inefficiency}_{it}/\text{Direct Effect}_{it}) \times 100\%$.[7]

Figure 3 illustrates the temporal evolution of these efficiency gains through monthly boxplots for the 2016m01–2017m12 period, while Table 3 provides their overall descriptive statistics. The results highlight the benefits of networks, as measured by interbank loans, in the Chilean industry. The median bank-period observation experiences an efficiency gain of approximately 20%, indicating a substantial reduction in operational costs attributable to network effects beyond its own idiosyncratic baseline. The considerable range of gains also shows significant heterogeneity in how different banks leverage, or are affected by, network interactions. Thus, our findings reinforce that interconnectedness not only influences the shape of the inefficiency distribution but also translates into economically meaningful improvements in cost efficiency for a significant portion of the Chilean banking sector.

Figure 3: Temporal Evolution of Network-Driven Efficiency Gains (%)

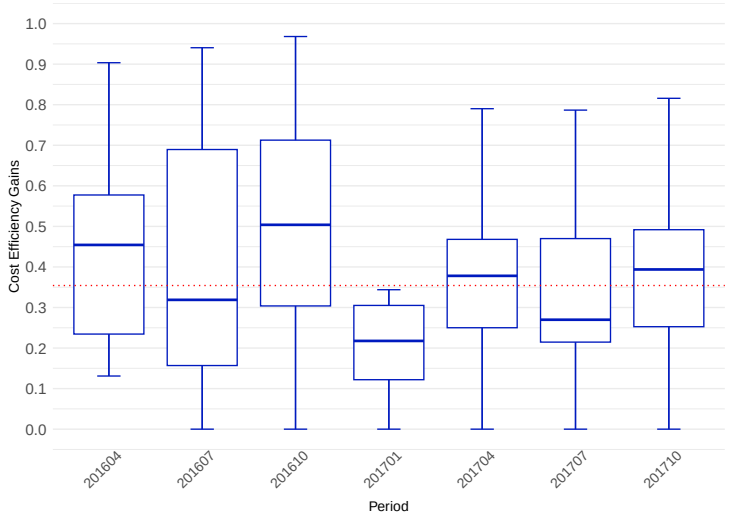

Notes: The figure presents a time series of monthly boxplots illustrating the distribution of Efficiency Gains for selected months over 2016m01–2017m12. Efficiency Gains are calculated as $(1 - \text{Total Inefficiency}_{it}/\text{Direct Effect}_{it})$. The horizontal dashed red line indicates the overall mean value of these gains across the sample period.

[7] This formulation stems from the decomposition Total Inefficiency = Direct Effect + Indirect Effect. Thus, the gain is $1 - \frac{\text{Direct Effect+Indirect Effect}}{\text{Direct Effect}}$. Since our estimated Indirect Effect is predominantly negative (indicating an efficiency improvement), this formula quantifies the positive percentage gain. For instance, if Direct Effect = 0.10 and Total Inefficiency = 0.07, the gain is $(0.10 - 0.07)/0.10 = 0.30$ or 30%. A small number of observations yielding extreme gain values (e.g., those initially above the 95th percentile), often resulting from division by Direct Effect values close to zero.

Table 3: Descriptive Statistics for Network-Driven Efficiency Gains

	Min.	1st Qu.	Median	Mean	3rd Qu.	Max.
Value	0.000	0.171	0.354	0.384	0.548	0.990

Note: The table reports descriptive statistics for the Efficiency Gain metric over the period 2016m01–2017m12, calculated as $(1 - \text{Total Inefficiency}_{it}/\text{Direct Effect}_{it})$. Total Inefficiency and Direct Effect components are derived from the stochastic cost frontier estimation.

4.4 Exploring Alternative Network Specifications as Robustness Checks and Channel Analysis

Our central finding of a negative network dependence parameter ($\hat{\rho} \approx -0.5$), suggesting that interconnectedness is associated with improved cost efficiency (lower inefficiency), aligns with several plausible economic mechanisms. Banks may experience heightened competitive pressures from their interconnected peers, incentivizing cost optimization. Alternatively, they might engage in learning or benchmarking behaviors, specifically 'negative benchmarking,' where banks actively observe and avoid operational inefficiencies exhibited by connected institutions.

A rigorous empirical disentanglement of these specific channels is complex and may be beyond the scope of this paper. Nevertheless, we leverage the richness of our administrative data (Form C-18) to explore how our findings hold up under alternative definitions of the network adjacency matrix (W_t). By systematically varying the underlying financial instruments and maturity categories that define the network, we can conduct comprehensive robustness checks of our main finding. Additionally, observing how the results change across these specifications allows us to conjecture about the potential mechanisms at play. For example, if network effects are stronger for certain types of obligations, it may suggest which kinds of interbank relationships are the primary conduits for these efficiency-enhancing spillovers.

4.4.1 Robustness to Network Definition by Maturity

We first exploit the maturity information in the C-18 data to construct three distinct versions of the adjacency matrix W_t, each based on the total value of obligations within a specific maturity category. Table 4 presents the estimation results for networks defined by: (1) 'Overnight/at sight' obligations, (2) obligations with maturity 'Up to one year', and (3) obligations with 'More than one year' maturity. The final column reports our baseline model, which uses all obligations combined.

We find no statistically significant network effect when interconnectedness is defined solely by at-sight obligations. This suggests that these very short-term exposures, likely reflecting daily operational liquidity management, may not be the primary channel for the strategic interactions that influence overall cost efficiency. Conversely, networks based on obligations with longer maturities exhibit strong, statistically significant, and negative dependence parameters. For obligations up to one year ($\hat{\rho} = -0.455^{***}$) and

those exceeding one year ($\hat{\rho} = -0.295^{***}$), interconnectedness is robustly associated with improved cost efficiency. The effect is largest in magnitude for the intermediate 'Up to one year' category. This may indicate that relationships with this maturity—which likely reflect core operational financing and risk management decisions beyond immediate liquidity needs—are particularly important conduits for competitive pressures or active benchmarking among banks.

Table 4: Model Results for Networks Defined by Obligation Maturity

Obligations	**Overnight/ at sight**	**Up to one year**	**More than one year**	**All Obligations (Baseline)**
Panel A. Interconnectedness parameter				
ρ	0.009	-0.455***	-0.295***	-0.542***
	(0.064)	(0.115)	(0.068)	(0.112)
Panel B. Cost frontier main parameters				
$\sigma_{\dot{v}}$	0.110***	0.101***	0.107***	0.102***
	(0.004)	(0.005)	(0.008)	(0.011)
$\sigma_{\dot{u}}$	0.016***	0.022***	0.019***	0.013***
	(0.005)	(0.005)	(0.004)	(0.005)
Controls in the Translog Cost Function	Yes	Yes	Yes	Yes
Time fixed effects	Yes	Yes	Yes	Yes
Observations	418	418	418	418

Notes: 1. The table reports the central results for the parameters in equations (1) and (2). The 'Controls in the Translog Cost Function' row indicates the inclusion of all first-order, second-order (squared), and interaction terms for outputs, input prices, and quasi-fixed inputs as specified in the translog cost function $TL(\boldsymbol{y}_{it}, \boldsymbol{p}_{it}, \boldsymbol{z}_{it}; \boldsymbol{\beta}^*)$ in equation (1). 2. Data: Chilean banking system (2016m1–2017m12). 3. Standard errors (in parentheses) computed via wild bootstrap. 4. *** significant at 1%; ** 5%; * 10%.

4.4.2 Robustness to Network Definition by Financial Instrument

We now explore the sensitivity of our findings by examining variations in the construction of the interbank network adjacency matrix (W_t) based on different combinations of financial instruments reported in Form C-18. Specifically, we construct alternative versions of W_t as follows: first, we define a network based exclusively on financial derivative contracts (*Derivatives Only*); second, we define an unsecured exposure network by subtracting collateral values from total obligations, thus isolating pure credit risk exposures (*Unsecured Exposures*); and third, we construct a traditional funding network using only term deposits (*Term Deposits Only*). Finally, we include our baseline network constructed from total obligations, which encompasses all instruments (*All Obligations (Baseline)*), for comparison.

Overall, the results presented in Table 5 strongly support the robustness of our central finding. The consistently significant and negative network dependence parameter across all specifications indicates that

the efficiency-enhancing effect is not driven by a single type of instrument. However, the results from these different specifications allow us to conjecture about the potential channels at play. For instance, the significant effect in the *Derivatives Only* network suggests that interactions related to risk management and hedging activities may serve as a channel for learning or benchmarking best practices. Similarly, the strong effect observed for *Unsecured Exposures* may highlight the role of heightened market discipline; the absence of collateral could intensify incentives for banks to actively monitor counterparts and to operate more efficiently to signal their creditworthiness. Finally, the finding for the *Term Deposits* network confirms that these efficiency-enhancing pressures are also present within the most traditional interbank funding markets, likely reflecting competitive forces. Collectively, these results suggest that the positive impact of interconnectedness on efficiency is a multifaceted phenomenon, driven by a combination of risk management benchmarking, heightened market discipline, and traditional competitive pressures.

Table 5: Model Results for Networks Defined by Financial Instrument Type

	Derivatives Only	**Unsecured Exposures**	**Term Deposits**	**All Obligations (Baseline)**
Panel A. Interconnectedness parameter				
ρ	-0.360***	-0.540***	-0.372***	-0.542***
	(0.064)	(0.111)	(0.117)	(0.112)
Panel B. Cost frontier main parameters				
$\sigma_{\dot{v}}$	0.107***	0.102***	0.106***	0.102***
	(0.013)	(0.012)	(0.005)	(0.011)
$\sigma_{\dot{u}}$	0.017***	0.013***	0.019***	0.013***
	(0.004)	(0.004)	(0.004)	(0.005)
Controls in the Translog Cost Function	Yes	Yes	Yes	Yes
Time fixed effects	Yes	Yes	Yes	Yes
Observations	418	418	418	418

Notes: 1. The table reports the central results for the parameters in equations (1) and (2). The 'Controls in the Translog Cost Function' row indicates the inclusion of all first-order, second-order (squared), and interaction terms for outputs, input prices, and quasi-fixed inputs as specified in the translog cost function $TL(\boldsymbol{y}_{it}, \boldsymbol{p}_{it}, \boldsymbol{z}_{it}; \beta^*)$ in equation (1). 2. Data: Chilean banking system (2016m1–2017m12). 3. Standard errors (in parentheses) computed via wild bootstrap. 4. *** significant at 1%; ** 5%; * 10%.

4.4.3 Other Specifications and Mechanisms (Ongoing Research)

(Further work is in progress to explore additional specifications, including changing the network directionality from borrower-to-lender to lender-to-borrower and employing alternative normalization methods. We are also developing formal tests to explore the roles of market competition and other network characteristics—such as centrality or concentration indices—in mediating the observed efficiency effects.)

5 (Preliminary) Conclusions

This paper research the influence of bank interconnectedness, as measured through the interbank lending market, on operational cost efficiency within the Chilean banking sector. Motivated by the extensive literature focusing primarily on the systemic risk and financial contagion aspects of financial networks, especially during crises, our study aimed to contribute to the less explored domain of how these network structures shape banking performance and efficiency during periods of relative economic stability.

Utilizing unique, transaction-level administrative data from the Chilean Financial Market Commission (CMF) for the period 2008–2020, we constructed time-varying network adjacency matrices (W_t) representing actual interbank lending relationships. To analyze these rich data, we employed a novel two-step Generalized Method of Moments (GMM) estimation strategy within a stochastic frontier analysis (SFA) framework. This approach integrated network dependencies via a spatial/network autoregressive parameter (ρ) in a flexible translog cost function, enabling the estimation of bank-specific cost inefficiencies while controlling for unobserved heterogeneity and network influences.

Our empirical analysis reveals robust evidence that interconnectedness is a statistically significant determinant of bank cost efficiency in Chile. We estimate an average network dependence parameter ($\hat{\rho}$) of approximately -0.5 , suggesting that, on average, network connections in the Chilean interbank market are associated with improved cost efficiency (i.e., lower cost inefficiency). Density estimates show a leftward shift in the distribution of total cost inefficiency relative to its idiosyncratic (Direct Effect) component. Quantifying this impact, our decomposition analysis reveals that network effects contribute to a significant "Efficiency Gain"; for the median bank-period observation, these network interactions account for a reduction in cost inefficiency of approximately 35 percentage points, relative to the bank's idiosyncratic baseline. These findings suggest that interbank networks may facilitate mechanisms such as competitive pressures or enhanced benchmarking opportunities, leading to tangible improvements in operational efficiency.

This study makes several contributions. Primarily, it extends empirical evidence beyond the traditional focus on systemic risks by providing quantitative insights into how interbank relationships concretely influence bank operational performance under normal economic conditions. Methodologically, our work demonstrates the application of advanced econometric techniques that effectively incorporate network dependencies with time-varying structures into stochastic frontier models using granular administrative data, specifically within a multi-output cost function context for banking. From a policy perspective, the findings highlight that interbank network structures are not only conduits of potential systemic risk but also critical elements influencing the efficiency and operational strength of the banking sector. Consequently, understanding and monitoring these network dynamics is essential for policymakers aiming to support robust, efficient, and stable financial systems that underpin broader economic health.

Given these preliminary results, avenues for future research include a deeper investigation into the specific channels through which interconnectedness translates into efficiency gains.

References

Acemoglu, D., A. Ozdaglar, and A. Tahbaz-Salehi (2015). Systemic risk and stability in financial networks. *American Economic Review 105*(2), 564–608.

Allen, F. and D. Gale (2000). Bubbles and crises. *The economic journal 110*(460), 236–255.

Baltagi, B. H. (2021). *Econometric Analysis of Panel Data* (6 ed.). Springer Texts in Business and Economics. Cham: Springer Nature.

Banerjee, A. V. (1992). A simple model of herd behavior. *The quarterly journal of economics 107*(3), 797–817.

Bikhchandani, S., D. Hirshleifer, and I. Welch (1998). Learning from the behavior of others: Conformity, fads, and informational cascades. *Journal of economic perspectives 12*(3), 151–170.

Brunetti, C., J. Harris, S. Mankad, and G. Michailidis (2019). Interconnectedness in the interbank market. *J. Financ. Econ. 133*(2), 520–538.

Chanci, L., S. C. Kumbhakar, and L. Sandoval (2024). Crime under-reporting in bogotá: A spatial panel model with fixed effects. *Empirical Economics 66*(5), 2105–2136.

Cobas, A., A. Maziotis, and A. Villegas (2024). Measurement of efficiency and its drivers in the chilean banking industry. *Plos one 19*(5).

Das, S., J. Mitchener, and A. Vossmeyer (2022). Bank regulation, network topology, and systemic risk: Evidence from the great depression. *Journal of Money, Credit and Banking 54*(5), 1261–1312.

Elhorst, J. P. (2010). Spatial panel data models. In M. M. Fischer and A. Getis (Eds.), *Handbook of applied spatial analysis*, pp. 377–407. Berlin, Heidelberg: Springer.

Elhorst, J. P. (2014). *Spatial Econometrics: From Cross-Sectional Data to Spatial Panels*. Springer Berlin Heidelberg.

Elliott, M., B. Golub, and M. O. Jackson (2014). Financial networks and contagion. *American Economic Review 104*(10), 3115–3153.

Freixas, X., B. M. Parigi, and J.-C. Rochet (2000). Systemic risk, interbank relations, and liquidity provision by the central bank. *Journal of money, credit and banking*, 611–638.

Glass, A. J., K. Kenjegalieva, and R. C. Sickles (2016). A spatial autoregressive stochastic frontier model for panel data with asymmetric efficiency spillovers. *Journal of Econometrics 190*(2), 289–300.

Glasserman, P. and H. P. Young (2016). Contagion in financial networks. *Journal of Economic Literature 54*(3), 779–831.

Gonçalves, S. and B. Perron (2020). Bootstrapping factor models with cross sectional dependence. *Journal of Econometrics 218*(2), 476–495.

Hou, Z., S. Zhao, and S. C. Kumbhakar (2023). The gmm estimation of semiparametric spatial stochastic frontier models. *European Journal of Operational Research 305*(3), 1450–1464.

Hughes, J. P., J. Jagtiani, L. J. Mester, and C.-G. Moon (2019). Does scale matter in community bank performance? evidence obtained by applying several new measures of performance. *Journal of Banking & Finance 106*, 471–499.

Jackson, M. and A. Pernoud (2021). Systemic risk in financial networks: A survey. *Annual Review of Economics 13*, 171–202.

Jondrow, J., C. K. Lovell, I. S. Materov, and P. Schmidt (1982). On the estimation of technical inefficiency in the stochastic frontier production function model. *Journal of econometrics 19*(2-3), 233–238.

Kumbhakar, S. and K. Lovell (2000). *Stochastic frontier analysis*. Cambridge university press.

Kumbhakar, S. C., H.-J. Wang, and A. Horncatle (2015). *A Practitioner's Guide to Stochastic Frontier Analysis*. Cambridge University Press.

Kutlu, L., K. C. Tran, and M. G. Tsionas (2020). A spatial stochastic frontier model with endogenous frontier and environmental variables. *European Journal of Operational Research 286*(1), 389–399.

LeSage, J. and R. K. Pace (2009). *Introduction to spatial econometrics*. Chapman and Hall/CRC.

Malikov, E., D. Restrepo-Tobon, and S. C. Kumbhakar (2015). Estimation of banking technology under credit uncertainty. *Empirical Economics 49*, 185–211.

Mammen, E. (1993). Bootstrap and wild bootstrap for high dimensional linear models. *The annals of statistics 21*(1), 255–285.

Mamonov, M., C. F. Parmeter, and A. B. Prokhorov (2024). Bank cost efficiency and credit market structure under a volatile exchange rate. *Journal of Banking & Finance 168*, 107285.

Manski, C. F. (1993). Identification of endogenous social effects: The reflection problem. *The review of economic studies 60*(3), 531–542.

Margaretic, P., R. Cifuentes, and J. G. Carreño (2021). Banks' interconnections and peer effects: Evidence from chile. *Research in International Business and Finance 58*, 101438.

Pace, K. and R. Barry (1997). Quick computation of spatial autoregressive estimators. *Geographical analysis 29*(3), 232–247.

Scharfstein, D. S. and J. C. Stein (1990). Herd behavior and investment. *The American economic review*, 465–479.

Sealey Jr, C. and J. Lindley (1977). Inputs, outputs, and a theory of production and cost at depository financial institutions. *The journal of finance 32*(4), 1251–1266.

Silva, T. C., M. da Silva Alexandre, and B. M. Tabak (2018). Bank lending and systemic risk: A financial-real sector network approach with feedback. *Journal of Financial Stability 38*, 98–118.

Silva, T. C., S. M. Guerra, B. M. Tabak, and R. C. de Castro Miranda (2016). Financial networks, bank efficiency and risk-taking. *Journal of Financial Stability 25*, 247–257.

Tabak, B. M., D. M. Fazio, and D. O. Cajueiro (2012). The relationship between banking market competition and risk-taking: Do size and capitalization matter? *Journal of Banking & Finance 36*(12), 3366–3381.

Tran, K. and M. Tsionas (2023). Semiparametric estimation of a spatial autoregressive nonparametric stochastic frontier model. *Journal of Spatial Econometrics 4*(1), 7.